American Mineralogist, Volume 93, pages 1245–1259, 2008

Forward modeling of the effects of mixed volatile reaction, volume diffusion, and formation of submicroscopic exsolution lamellae on calcite-dolomite thermometry

Thomas Müller,[1,*] Lukas P. Baumgartner,[1] C. Tom Foster Jr.,[2] and Gregory T. Roselle[3]

[1]Institute of Mineralogy and Geochemistry, University of Lausanne, CH-1015 Lausanne, Switzerland
[2]Department of Geosciences, University of Iowa, Iowa City, Iowa 52242, U.S.A.
[3]Sandia National Laboratories Carlsbad Programs Group, Carlsbad, New Mexico 88220, U.S.A.

Abstract

This paper reports the results of several thousand analyses of the Mg content of calcite from 31 samples from the Ubehebe Peak contact aureole, Death Valley, California. All data reported are from metamorphic calcite formed during mixed volatile-mineral reactions in which dolomite remained in the rock. The Mg content generally increases toward the intrusive contact and bend with increasing temperature, but it varies strongly. Indeed, probability distributions for each sample are near Gaussian, possess a relatively small skewness (–1.72 to 3.32), and a variance that is a multiple of the estimated measuring uncertainty. These findings complicate direct application of the Mg content in calcite for use as an accurate thermometer.

The purpose of the study presented in the second part of the paper is to explore the significance of these systematic variations of Mg composition of calcite to aid the interpretation of contact metamorphic temperatures recorded in carbonates. We developed forward models to evaluate the effect of growth zoning, volume diffusion, and the formation of submicroscopic exsolution lamellae (<1 μm) on the measured Mg distribution in individual calcite crystals and compared the modeling results to the field data. Modeled Mg distributions were transformed into histograms by taking into account intersection probabilities and random microprobe analyses. Modeling results reveal that the original prograde Mg zoning in calcite crystal will be reset if the calcite crystal is assumed to grow slowly along a prograde path. Original low-Mg compositions can only be preserved if the entire grain forms over a small temperature interval, as can be expected for infiltration-driven mineral reactions. It is shown that all three mechanisms combined give an adequate model for the Mg-content data. We demonstrate that Mg distributions in calcite grains of the Ubehebe Peak contact aureole are the consequence of rapid crystal growth in combination with diffusion and exsolution.

Keywords: Calcite-dolomite thermometry, contact metamorphism, Ubehebe Peak, mineral growth, fluid infiltration

Introduction

Calcite-dolomite thermometry is commonly used to estimate peak temperatures in metamorphic carbonates. It is based on the temperature dependence of Mg exchange between calcite and dolomite, which has been experimentally calibrated (Goldsmith and Heard 1961; Powell et al. 1984; Anovitz et al. 1987). The principles and application of solvus thermometry were thoroughly reviewed by Essene (1983). Successful applications (Holness et al. 1991; Masch and Heuss-Abichler 1991; Cook and Bowman 1994; Letargo et al. 1995; Ferry 1996a) found temperatures from calcite-dolomite pairs in agreement with those obtained for silicate-carbonate equilibria. These studies concluded that the calcite-dolomite thermometer recorded peak metamorphic conditions. Rathmell et al. (1999) compared garnet-biotite, calcite-graphite, and calcite-dolomite thermometry in the Grenville Orogen in Canada. Although calcite-dolomite pairs yielded lower temperatures in comparison with the other two thermometers, resulting temperatures agreed quite well, if care was taken to use only calcite grains with no visible dolomite exsolution.

Maximum temperature-distance profiles obtained from calcite-dolomite thermometry in contact metamorphic terranes are mostly consistent with the spatial distribution of prograde metamorphic reactions given by equilibrium phase diagrams (Cook and Bowman 1994; Ferry 1996a; Roselle 1997). However, samples at similar distances from a pluton (Fig. 1) commonly exhibit differences in calculated temperatures of up to several hundred degrees (Cook and Bowman 1994; Roselle 1997; Ferry 2001), although they should have experienced the same temperature. This problem becomes more puzzling when one looks at how the temperatures were obtained. Typically a large number of microprobe analyses on different calcites are obtained from a single thin section. Figure 2 shows histograms of measured data that exhibit large variations in X_{Mg}, which indicate a range of up to 200 °C within a single sample. Furthermore, no simple concentric zoning patterns are observed within single grains. As a result, the interpretation of such data and thus the determination

* Present address: Institut für Mineralogie, Geologie und Geophysik, Ruhr-Universität Bochum, D-44780 Bochum, Germany. E-mail: Thomas.H.Mueller@rub.de

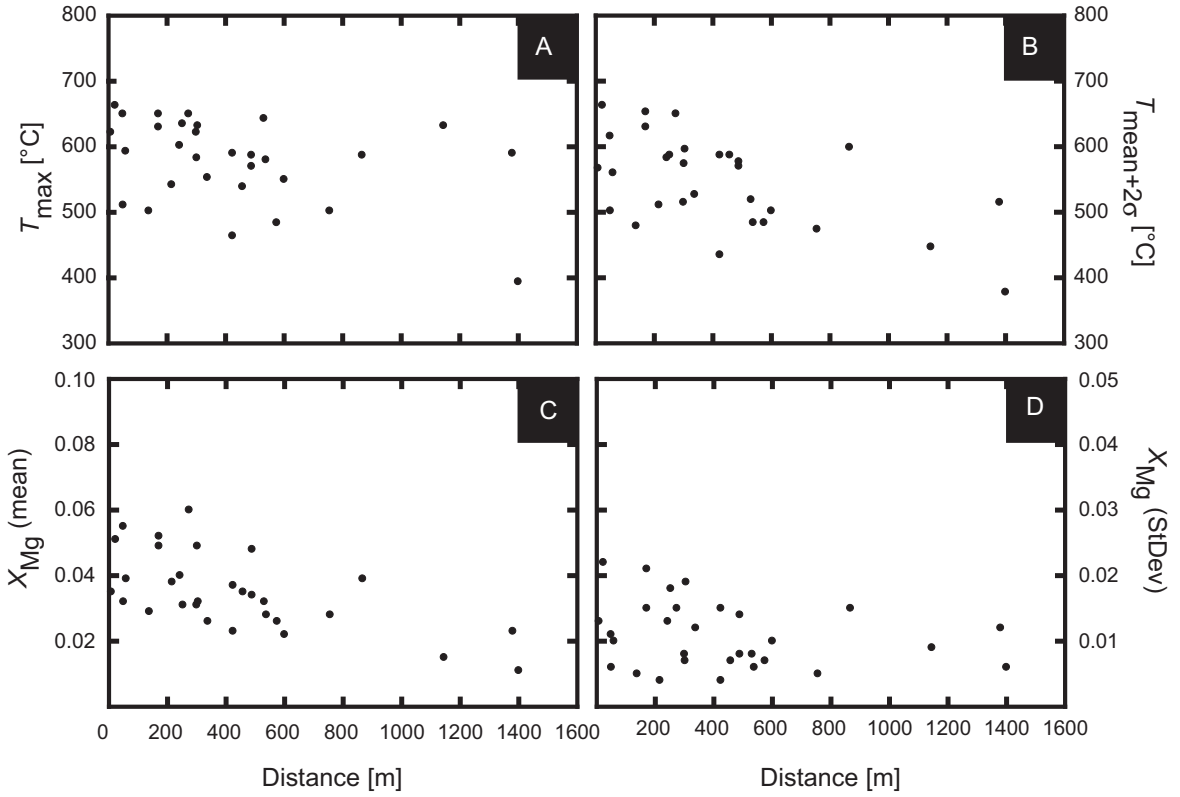

FIGURE 1. Calcite-dolomite thermometry data for 31 samples from the Ubehebe Peak contact aureole plotted as a function of distance to the intrusive contact. Temperatures (= X_{Mg}) increase with increasing proximity to the contact as expected, but note the large difference in temperatures for samples collected at the same distance. (**a**) Temperatures calculated using the highest measured X_{Mg} value of a sample. (**b**) Temperatures calculated using the mean X_{Mg} value of a sample plus two times the standard deviation following the approach of Roselle (1997). (**c**) Measured mean X_{Mg} values as a function of the distance from the contact. (**d**) Standard deviations in measured X_{Mg} contents. Note that the variations become larger with decreasing distance from the magmatic contact.

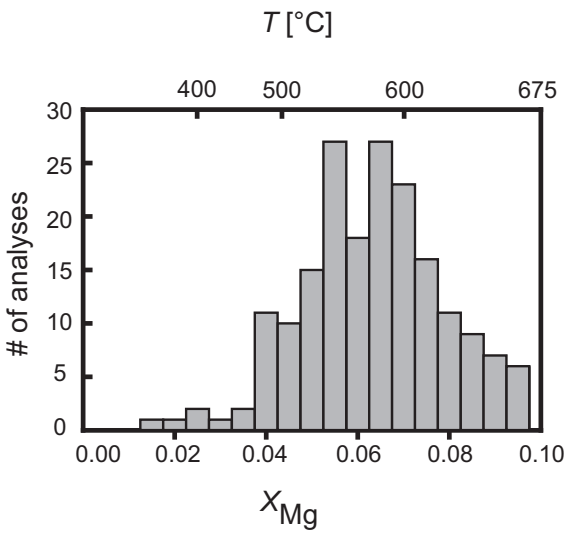

FIGURE 2. Histogram of measured X_{Mg} values of sample 94-JUB-24 from the Ubehebe Peak aureole. The variations in the Mg content of calcite correspond to a variation in temperature of more than 200 °C.

of peak metamorphic temperatures are problematic. Investigators have developed different approaches to calculate temperatures from calcite-dolomite thermometry data sets (Holness et al. 1991; Masch and Heuss-Abichler 1991; Cook and Bowman 1994; Roselle 1997; Ferry 2001). All of these approaches imply that variations are mainly due to partial resetting.

During the last decade, several studies on metamorphic crystal growth highlighted the importance of kinetics (Holness et al. 1991; Carlson et al. 1995; Ferry and Gerdes 1998; Lasaga 1998; Carlson 2002; Müller et al. 2004). In rapid-heating environments such as contact aureoles, overstepping of equilibrium temperature as well as fluid composition can potentially have large effects on the crystallization history. Hence, it is possible that a mixed-volatile reaction path as well as retrogression could be responsible for the observed variations in X_{Mg} of calcite grains.

In this study, we present detailed calcite-dolomite thermometry data on multiple scales from the Ubehebe Peak contact aureole (U.S.A.). To understand the observed systematic scatter of measured Mg-contents of calcite and to clarify the interpretation of resulting metamorphic temperatures, we have developed forward models. These models evaluate the effect of growth zoning, volume diffusion, and the formation of submicroscopic exsolution lamellae (<1 μm) on the measured Mg concentrations. The results are then compared to the Ubehebe Peak data set.

GEOLOGICAL SETTING, SAMPLES AND ANALYTICAL METHODS

Geologic setting

The quartz monzonitic Ubehebe Peak intrusion is part of a series of alkaline intrusions forming the Hunter Mountain Batholith (McAllister 1955, 1956; Roselle et al. 1999), located in Death Valley National Park, California. Its age is 173 ± 1 Ma (Roselle 1997). The Ubehebe Peak contact aureole was formed in a sequence of Paleozoic sediments, consisting mainly of siliceous dolomite. The units in the Ubehebe Peak area were thrusted and folded prior to intrusion during a Late Permian to Middle Triassic regional metamorphic event. Intrusion caused local deformation of the host rock and some calcite lattice orientation fabric (Evermann 1998; Müller 2002).

Contact metamorphism caused the formation of tremolite, forsterite, and finally periclase with increasing proximity toward the contact in the siliceous dolomite units (Roselle 1997; Roselle et al. 1997, 1999). Locally, retrograde talc is found in the outer part replacing tremolite.

Rare diopside can be found together with forsterite and/or tremolite in dolomitic marbles in the outer part of the forsterite zone. The absence of a well-defined diopside zone indicates the presence of H_2O-rich fluids during contact metamorphism (Ferry and Dipple 1992). Clearly lowered $\delta^{18}O$ and $\delta^{13}C$ values indicative of fluid infiltration were found in only 20–28% in the large data set of 357 samples (Roselle et al. 1999). The authors explained those low percentages of infiltrated samples with the presence of fluid channels and a relatively small amount of fluid flow.

Samples

A total of 31 samples of siliceous dolomite were selected for analysis. They are distributed across the Ubehebe Peak aureole. A detailed investigation focusing on variation at the thin section scale was initiated within one lithologic horizon. The so-called "gray layer" (Roselle 1997) was chosen because of its simple mineralogy. It contains only dol + cal ± fo ± tr (all mineral abbreviations after Kretz 1983). Mineral assemblages of the three samples used from this horizon are listed in Table 1. The unmetamorphosed protolith for this layer is dol + qtz with an average modal percent of approximately 90% dol and 10% qtz.

The sample 94-JUB-24 measured in this study was also used to investigate variations in calcite chemistry in the vicinity of single olivine porphyroblasts. Besides a few tremolite crystals, this sample contains large, tabular olivine porphyroblasts with a long axis of about 1 mm. The porphyroblasts are surrounded by calcite halos having a width of about 200–400 µm. Olivines and their calcite halos in this sample are the products of either the stable reaction:

1 tremolite + 11 dolomite → 8 forsterite + 13 calcite + 1 H_2O + 9 CO_2 (1)

or, as proposed by Müller et al. (2004), the meta-stable reaction:

2 dolomite + 1 quartz → 1 forsterite + 2 calcite + 2 CO_2 (2)

However, all calcite in this sample is metamorphic in origin and was formed during the olivine- and the tremolite-forming reactions, respectively. None of the samples selected contained calcite crystals with visible dolomite exsolution.

TABLE 1. Mineral modes of samples in the gray layer used for detailed investigations

Sample	Distance to contact (m)	Metamorphic zone	Modal percentage			
			cal	dol	tr	ol
94-JUB-24	274	ol	39.2	42.4	0.3	18.1
94-JUB-46	302	ol	29.2	52.7	0.0	18.1
94-JUB-19	489	ol	22.1	64.7	0.5	12.7

ANALYTICAL METHODS

To obtain a temperature-distance profile at the aureole scale (Fig. 1), 31 samples containing coexisting calcite and dolomite were selected and the X_{Mg} content of calcite grains was determined for 30–120 spot analyses distributed across the thin section.

Analyses were obtained with the Cameca SX50 electron microprobe at the Universities of Lausanne and Wisconsin. Cup current was set at 6 nA and accelerating voltage at 15 kV, with a beam diameter of 15 µm. Representative calcite analyses from the tremolite, forsterite, and periclase zone are shown in Table 2. A counting time of 60 s was used for Ca and Fe, and 120 s for Mg and Mn. Standards were natural calcite (Ca), dolomite (Mg), siderite (Fe), and pyrophanite (Mn). The typical confidence limit for the Mg analyses is about 0.06 wt% (equals X_{Mg} ~ 0.002), resulting in an error of about ±5 °C for the calculated temperatures in the range of interest. Analyses were corrected using the PAP correction and subsequently normalized to one cation. Temperatures were calculated using the calibration of Anovitz et al. (1987). Since all measured calcite grains do not contain any significant amounts of Fe and Mn (Table 2), no correction were needed for these elements for the temperature calculation.

A more detailed investigation of three samples from the "gray layer" was performed, where the chemical composition of 185–290 equally distributed points on calcite grains was measured for each thin section. X-ray element maps of Ca, Mg, and Si were made for the entire thin sections. Combined RGB-images were created with imaging software "-Aphelion" using the peak count for each element. This procedure allows identification of mineral phases in the vicinity of measured points.

Central cuts of 5 olivine porphyroblasts were made using a diamond wire saw with a 130 µm wire, resulting in a precision of ±15–50 µm for the different cuts. The Mg content of the surrounding calcite halos were measured by 200–300 spot analyses, including multiple analyses on individual grains.

RESULTS

Aureole scale

Results of calcite analyses are summarized in Table 3 for the 31 samples. The measured values of X_{Mg} of calcite range between 0.008 and 0.095. The temperature-distance profile through the aureole shows a clear trend of higher temperatures

TABLE 2. Representative calcite analyses from the Ubehebe Peak contact aureole

	per zone 94-UB-108	fo zone 94-JUB-24	tr zone 94-UB-118
CaO	51.43	51.94	53.87
MgO	2.80	2.39	1.90
MnO	0.00	0.02	0.00
FeO	0.00	0.01	0.01
Mineral formula			
Ca(CO3)	0.930	0.939	0.953
Mg(CO3)	0.070	0.060	0.047
Fe(CO3)	0.000	0.000	0.000
Mn(CO3)	0.000	0.000	0.000

Notes: Analyses were obtained using a 15 keV, 6 nA, 15 µm beam. Mineral formulae calculated based on (Ca + Mg + Fe + Mn) = 1.

TABLE 3. Summary of calcite analyses for carbonate samples of the Ubehebe Peak contact aureole

Sample	Distance to contact (m)	Metamorphic zone	No. of analyses	X_{Mg}					Peak temperature (°C)		
				min	max	mean	StDev	skewness	Calculated using the lowest X_{Mg} value	Calculated with mean + 2σ	Calculated using the highest X_{Mg} value
94-UB-107	8	per	100	0.012	0.079	0.035	0.013	–0.21	225	567	622
94-UB-105	23	per	47	0.016	0.095	0.051	0.022	0.14	301	663	663
94-UB-92	49	fo	81	0.020	0.090	0.055	0.011	–0.16	350	616	650
02-TUB-10	50	fo	51	0.021	0.046	0.032	0.006	0.61	360	502	511
94-UB-108	59	per	97	0.012	0.069	0.039	0.010	0.48	225	560	593
94-UB-54	138	fo	44	0.018	0.044	0.029	0.005	1.05	328	479	502
92-IN-31	171	fo	30	0.019	0.082	0.052	0.015	–0.68	339	630	630
92-IN-32	171	fo	31	0.019	0.090	0.049	0.021	0.11	339	653	650
94-UB-71	216	fo	97	0.023	0.054	0.038	0.004	–0.17	378	511	542
94-JUB-25	243	fo	37	0.016	0.072	0.040	0.013	0.66	301	583	602
94-UB-122	253	fo	52	0.008	0.084	0.031	0.018	0.48	65	587	635
94-JUB-24	274	fo	185	0.015	0.090	0.060	0.015	–0.33	286	650	650
02-TUB-48	300	fo	103	0.016	0.079	0.031	0.008	2.55	301	515	622
94-JUB-46	302	fo	290	0.025	0.066	0.049	0.007	–0.90	394	574	583
94-UB-102	305	fo	51	0.008	0.083	0.032	0.019	0.61	65	596	632
94-JUB-27	338	fo	37	0.011	0.057	0.026	0.012	1.34	198	527	553
94-JUB-30	424	fo	21	0.019	0.068	0.037	0.015	0.49	339	587	590
94-JUB-30	424	fo	286	0.012	0.036	0.023	0.004	0.09	225	435	464
94-UB-88	458	fo	88	0.017	0.053	0.035	0.007	0.42	315	587	539
94-JUB-19	489	fo	50	0.015	0.062	0.034	0.014	0.63	286	570	570
94-JUB-19	489	fo	208	0.008	0.067	0.048	0.008	–1.72	65	577	587
94-UB-119	531	fo	97	0.009	0.087	0.032	0.008	1.22	121	519	643
94-UB-76	538	fo	100	0.007	0.065	0.028	0.006	–0.41	N.A.	484	580
95-UB-196	575	fo	21	0.011	0.040	0.026	0.007	–0.15	198	484	484
94-UB-87	600	fo	49	0.003	0.056	0.022	0.011	0.27	N.A.	502	550
94-UB-118	756	tr	99	0.012	0.044	0.028	0.005	0.11	225	474	502
94-UB-98	867	tr	25	0.006	0.067	0.039	0.016	1.08	N.A.	599	587
02-TUB-16	1145	tr	134	0.002	0.083	0.015	0.009	3.32	N.A.	447	632
94-UB-134	1380	tr	35	0.003	0.068	0.023	0.012	1.26	N.A.	515	590
02-TUB-47b	1400	tr	95	0.002	0.025	0.011	0.006	–0.36	N.A.	378	394

Note: Corresponding temperatures were calculated using the calibration of Anovitz et al. (1987).

with increasing proximity to the contact (Fig. 1). However, as previously stated by Ferry (2001), the variations for samples of similar distances from the intrusion are clearly too high to be explained by analytical uncertainties only (Fig. 2). Interestingly, the heterogeneity becomes larger with increasing metamorphic grade, i.e., toward the contact (Roselle 1997; Ferry 2001). This is confirmed by the data in this study (Figs. 1 and 3).

Histograms of the measured X_{Mg} data exhibit near Gaussian shapes (Figs. 2 and 3) for each individual sample. To facilitate comparison between samples and to highlight the shape of the X_{Mg}-value distribution, we have transformed the histograms to probability histograms by dividing through by the number of analyses of each sample (Fig. 3). Highest grade samples (e.g., 94-JUB-24) show the greatest heterogeneity with a one-sigma variation of about 0.015. The typical mean X_{Mg}-value representing samples of the forsterite zone is 0.006 (~565 °C) and the skewness of the distributions ranges between –1.72 and 3.32. Samples 94-JUB-46 and 94-JUB-19 from the forsterite zone exhibit similar variations in composition. However, the peak height of the mean value of the slightly higher grade sample (94-JUB-46) is more pronounced. The calculated temperatures are nearly equal for these two samples. The mean value for samples of the tremolite zone is typically about X_{Mg} = 0.045 with a one-sigma variation of 0.01. The distributions still exhibit near-Gaussian shapes, although the skewness increases slightly to about –1.0.

One of the goals of this study was to evaluate the statistical robustness of the calcite-dolomite thermometry on different scales. To that end, a second thin section of sample 94-JUB-19, which was already measured by Roselle (1997), was prepared. Whereas Roselle (1997) measured 50 points, a total of 208 equally distributed points were measured for this study. Using the same approach for temperature calculation yields 571 °C (Roselle 1997) and 581 °C for this study, respectively. Hence, they are in excellent agreement.

Thin-section-scale variations

A total of 185 to 290 calcite analyses, distributed on a grid were obtained on three thin sections (Table 1 and 3). These measurements reveal the presence of domains of higher and lower values of Mg content. The domains are most obvious in the highest grade sample studied here (94-JUB-24). X-ray element maps were used to identify mineral phases. Domains of higher Mg content contain abundant forsterite, and an excellent correlation is observed with accumulations of large forsterite porphyroblasts (Fig. 4). In contrast, lower Mg contents were found around tremolite crystals. The same observation can be made for the other three samples.

Porphyroblast-scale variations

The sample with the largest variations (94-JUB-24) was chosen for an in-depth investigation. Between 92 and 351 spot analyses were obtained on five calcite halos surrounding central cuts of forsterite porphyroblasts (Table 3). Histograms of the analyses are shown in Figure 5. The mean values for the Mg contents for each halo vary between X_{Mg}= 0.054 and 0.066.

Indeed, the range of measured X_{Mg} values is as large as that observed in the bulk rock measurements (Tables 3 and 4). The skewness of the distribution in the histograms is again small, with values of about –0.5.

Multiple analyses within single calcite grains reveal that several grain boundaries have lower X_{Mg} values (Fig. 6). These grain boundary rims are typically 20–30 μm in thickness. Nevertheless, not all grains are systematically zoned, and single analyses on calcite grains can exhibit surprisingly high values (Fig. 6). But an inverse trend of systematically increasing X_{Mg} values toward the calcite rims was not observed.

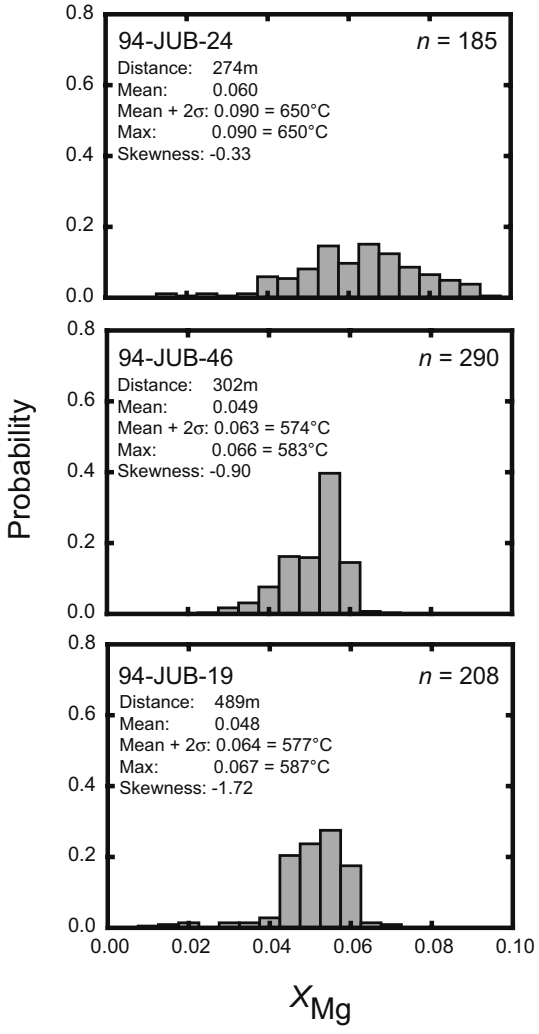

FIGURE 3. Probability histograms based on number of measured X_{Mg} values for samples of the "gray layer." Samples 94-JUB-19 and 94-JUB-46 belong to the tremolite zone and sample 94-JUB-24 belongs to the forsterite zone, respectively. Heterogeneity becomes larger with increasing proximity to the igneous contact. Note the near-Gaussian shape for all histograms.

DISCUSSION OF THE RESULTS

The general trend of higher Mg content and hence, higher temperatures, in the vicinity of the intrusion confirm that calcite does indeed record metamorphic temperatures because calcite near the contact clearly recorded higher temperatures. However, the presence of large ranges in X_{Mg} within each sample makes interpretation of the measured data problematic.

Different approaches were adopted to determine the metamorphic peak temperature for individual samples. Several studies (Holness et al. 1991; Masch and Heuss-Abichler 1991; Cook and Bowman 1994) suggested using the highest measured X_{Mg} value, assuming that all variation is due to partial retrograde re-equilibration. The use of this method requires that all analyses that are the result of mixtures between calcite and dolomite—due to grain boundary intersection out of the plane of the surface of the polished section—can be estimated. Hence, Roselle (1997) proposed another method which uses the Mg content corresponding to a value 2σ above the mean value of the sample. Calculated temperatures using these two methods for the samples of the Ubehebe Peak are shown in Table 3. Comparing the two approaches yield no significant differences in the resulting temperature estimates, but the approach of Roselle (1997) inherently yields slightly lower temperatures. Nevertheless, both approaches tend to underestimate the metamorphic peak temperature. In addition, they need large data sets, either to find the highest X_{Mg} value in the thin section or to adequately define the shape of the distribution. The degree of underestimation and therefore the error of the calculated temperatures would then depend on the extent of alteration. Consequently, Ferry (2001) proposed to only use calcite inclusions in forsterite. Retrograde equilibration with dolomite should not significantly affect these isolated calcite grains. In fact, this method results in higher temperatures in comparison with the previously discussed methods. This approach could unfortunately not be tested for the Ubehebe Peak aureole, since forsterite from this aureole does not generally contain any isolated calcite inclusions. Although inclusions can be found, they are not isolated, as was demonstrated by Müller et al. (2004) using X-ray tomography.

The correlation of elevated temperatures in calcite grains near forsterite porphyroblasts and lower temperatures in the vicinity

TABLE 4. Summary of calcite analyses surrounding olivine porphyroblasts in metamorphic carbonates of the Ubehebe Peak contact aureole

Sample	No. of analyses	X_{Mg}					Peak temperature (°C)		
		min	max	mean	StDev	skewness	Calculated using the lowest X_{Mg} value	Calculated with mean + 2σ	Calculated using the highest X_{Mg} value
94-JUB-24 (whole rock)	185	0.015	0.090	0.060	0.015	–0.33	286	650	650
Porpyhroblast 1a	93	0.023	0.093	0.065	0.012	–0.16	378	648	658
Porpyhroblast 1c	220	0.027	0.092	0.060	0.010	0.17	409	624	655
Porpyhroblast 4a	225	0.017	0.091	0.055	0.013	0.51	315	627	653
Porpyhroblast 4b	351	0.019	0.096	0.066	0.012	–0.39	339	650	665
Porpyhroblast 5b	255	0.020	0.093	0.053	0.013	0.23	350	622	658

Note: Corresponding temperatures were calculated using the calibration of Anovitz et al. (1987).

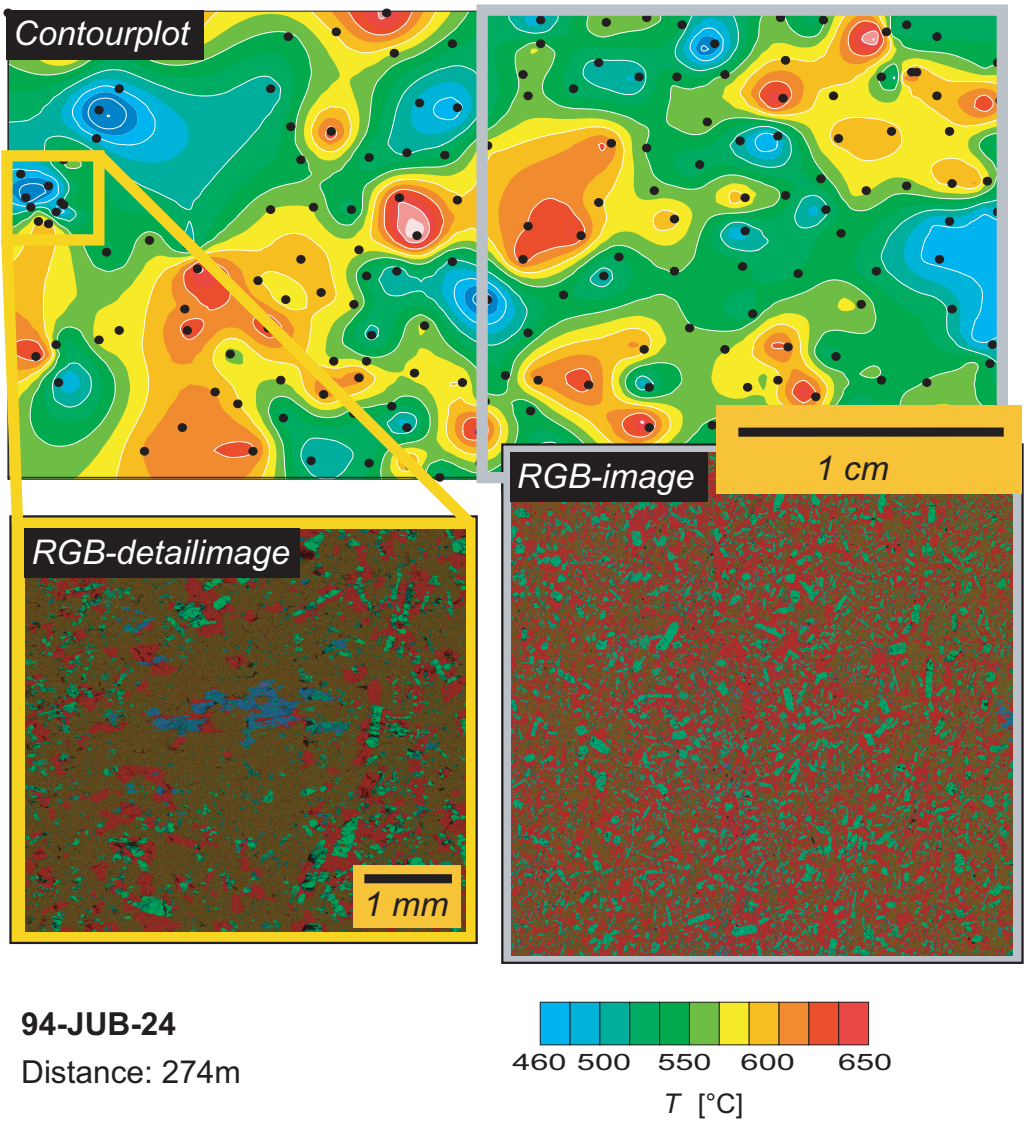

FIGURE 4. Contour plot of the temperatures obtained from regularly spaced calcite-analyses using values of X_{Mg}. Black dots mark the measured points. RGB images of the thin section were obtained by combining element *X*-ray maps (R = Ca*K*α; G = Mg*K*α, B= Si*K*α) allow us to identify the mineral phases in the section (calcite = red, forsterite = green, and tremolite = blue). Domains of lower X_{Mg} values, corresponding to lower apparent temperatures, are found near tremolite (RGB-detail image), whereas domains of higher temperatures are found near large forsterite porphyroblasts. (To print in journal, images are CMYK.)

of tremolite crystals is in agreement with temperature differences maintained by the formation of the calcite grain during mixed-volatile reactions. Tremolite, regardless of the timing of its formation (prograde or retrograde), will form at lower temperatures compared to forsterite porphyroblasts, unless the composition of the fluid phase is extremely water-rich (Fig. 7). In addition, the range of average temperatures obtained from domains near tremolite or forsterite grains are compatible with the temperature ranges predicted for the tremolite- and forsterite-forming reactions by the phase diagram calculated at 1.5 kbar (Fig. 7). This agreement suggests that at least part of the measured variations in X_{Mg} in calcite reflects the consequences of progressive growth of calcite accompanying the formation of forsterite and tremolite due to dolomite break down.

With this in mind, we tried to gain further insight into olivine porphyroblast growth. The growth of a porphyroblast occurs during a time span beginning with its nucleation and subsequent growth, as long as temperature and material supply allow continuous growth (Joesten 1991). Consequently, a growing porphyroblast will be accompanied by a series of newly formed calcite as reactions 1 or 2 proceed. Assuming that a tabular forsterite crystal grows from its center toward the rims, calcite in the vicinity of the center reflects the earliest formed calcite grains whereas calcite near the rims should have been formed during the last growth stage of the porphyroblast. Systematic trends of increasing or decreasing Mg content would potentially indicate whether the porphyroblast grew during heating, cooling, or both. To document any such trends, we divided the calcite

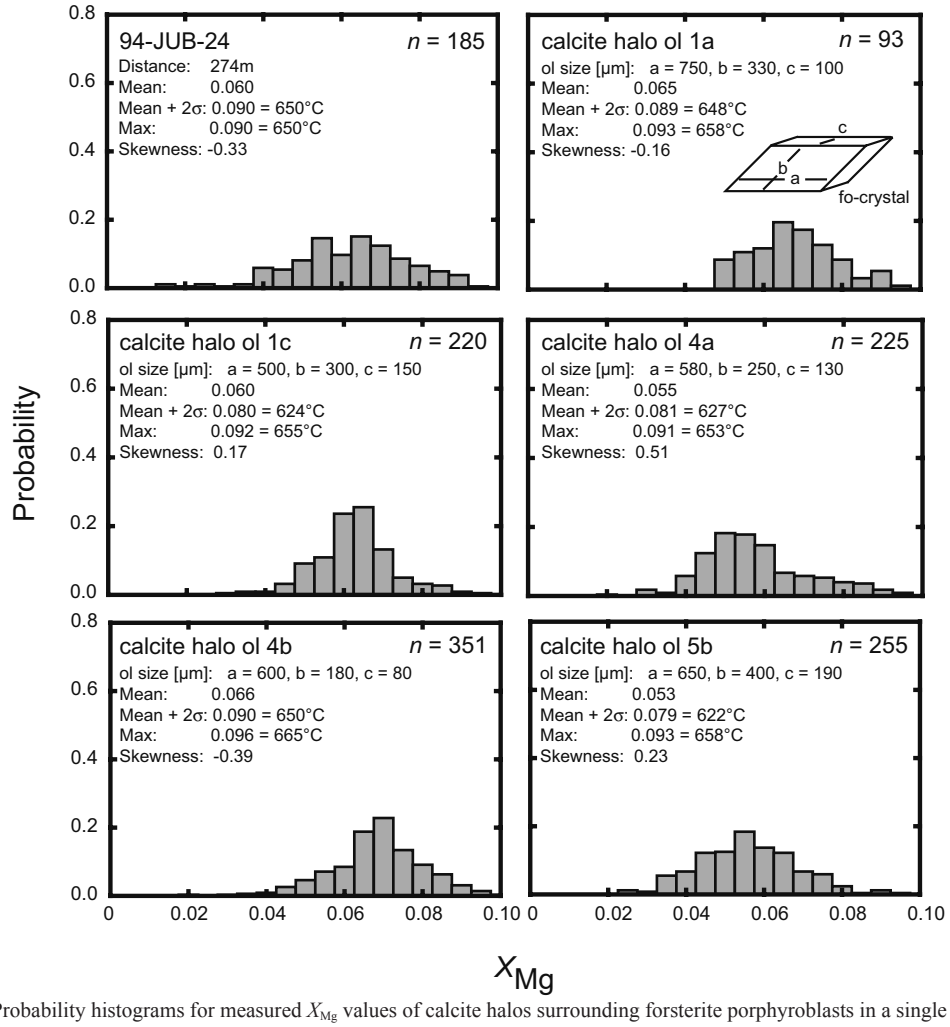

FIGURE 5. Probability histograms for measured X_{Mg} values of calcite halos surrounding forsterite porphyroblasts in a single sample. Note that all olivine crystals were centrally cut. All histograms exhibit a near-Gaussian shape with a similar variation compared to the analyses of the entire thin section.

halo into squares containing approximately the same number of measurements. The average values of each square are similar for a porphyroblast (Fig. 8a). The same is true if the analyses for each single calcite grain in the halo are averaged (Fig. 8b). The fact that all averaged grains and squares exhibit similar temperatures is interpreted as either the result of partial resetting of the calcite composition or of rapid growth rates, resulting in the growth at roughly constant temperature. Variations of the Mg content measured within single calcite grains (Fig. 6), as well as the absence of systematic zoning patterns, favor the kinetic interpretation, which implies high reaction rates and thus relatively high reaction affinities that allow the forsterite to grow rapidly.

FORWARD MODELING

The detailed data presented here as well as data from previous studies all suggest that these measured variations in Mg content of calcite grains reflect some combination of processes, including both growth of calcite and subsequent modification by diffusion. The very similar variations observed on every scale yield two important consequences: (1) variations are due to processes acting on single grains, and (2) these processes are

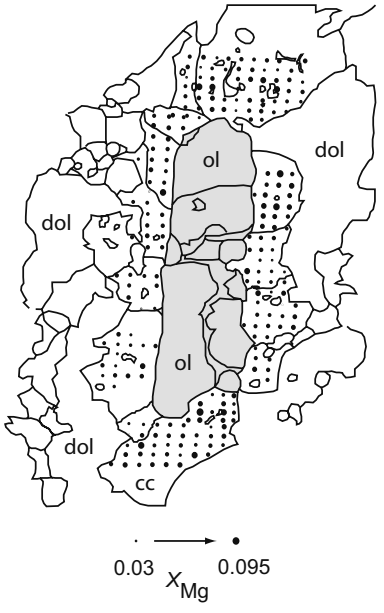

FIGURE 6. Measured Mg-content of calcite grains surrounding an olivine porphyroblast. The size of the black spots is proportional to the X_{Mg} value. No systematic spatial trends of X_{Mg} distribution or concentric zoning patterns are apparent.

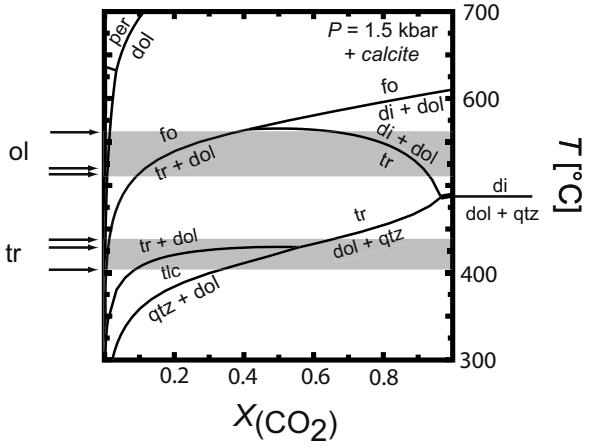

Figure 7. A phase diagram for the system CaO-MgO-SiO_2-H_2O-CO_2 for calcite saturation calculated at 1.5 kbar using the thermodynamic data set of (Holland and Powell 2001). Arrows on the left side mark temperatures calculated for the average of calcite analyses in the vicinity of olivine and tremolite crystals, respectively. Temperature recorded by the calcite compositions agree with the *T* conditions of the reaction that forms the adjacent silicate phase. Diagram calculated using the Perplex-software package (Connolly and Kerrick 1987).

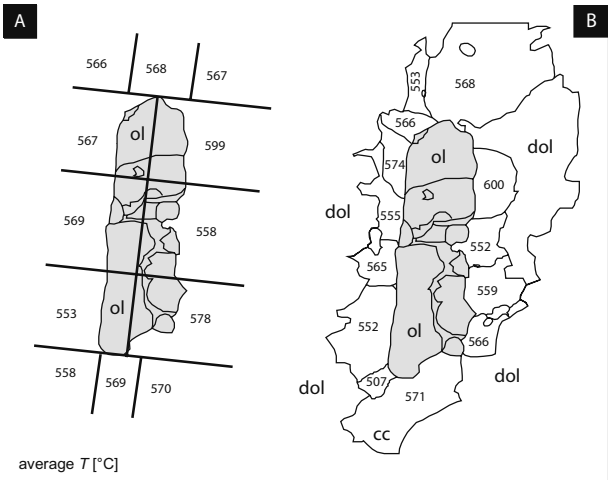

Figure 8. (**a**) Average temperature calculated for each square indicated for a calcite halo surrounding olivine. No trend of increasing or decreasing temperature can be seen. (**b**) Averaged temperature of each individual calcite grain for the same calcite halo.

generally applicable to all samples and are a function of changing *P-T-t* conditions. We present some forward models to evaluate the effect of growth zoning, volume diffusion, and retrograde formation of submicroscopic exsolution lamellae on the Mg content measured by microprobe analyses in calcite.

Calcite growth by mixed volatile reaction in a closed system

Several studies have correlated carbonate zoning patterns with isotopic compositions or trace-element variations (Reeder 1992; Watson 1996, 2004). In addition, Wada and Suzuki (1983) described Mg-zoning patterns in calcite grains. To quantify potential zoning patterns, we developed a model in which spherical calcite crystals grew due to reaction 1 along a predefined *T-t* path.

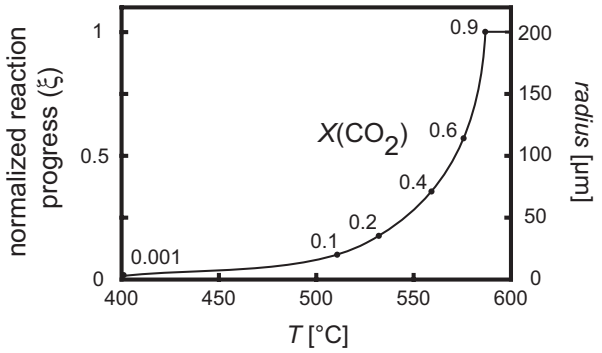

Figure 9. Relationship between model parameters describing the growth of a spherical calcite crystal grown by the reaction 11 dol + 1 tr ↔ 8 ol + 13 cc + 9 CO_2 + H_2O in a closed system, with a porosity of 1% filled with fluid.

The *T-t* path is defined by thermal modeling for the Ubehebe Peak intrusion (Roselle 1997), based on temperatures obtained by a smaller set of calcite-dolomite thermometry (Table 3) and phase petrology. Based on the depth of intrusion and a prior regional metamorphic event, the temperature of the quartz-monzonitic intrusion was estimated to be 750 °C, and the initial temperature of the host rock was set to 350 °C. In addition to the calcite-dolomite thermometry data, the thermal model was set to fit to the spatial extent of periclase observed in the aureole. The formation of periclase requires temperatures above 605 °C at water-rich conditions (Fig. 7). Therefore, the thermal model requires convection in the magma chamber. To compare modeling results with our field data, we use the modeled *T-t* path for sample 94-JUB-24, located 280 m from the intrusive contact. We further assumed that material supply is not limited and thus the grain boundaries of calcite crystals are in local equilibrium with dolomite at any time during the growth of calcite. Calculations were performed for 1 cm^3 rock volume, and a pore space of 1% is assumed. Starting composition of fluid in the pore space was set to nearly pure water with an initial X_{CO_2}-value of 0.001, i.e., 1.0^{-10} moles of CO_2 and 2.85^{-4} moles of H_2O, respectively. The starting rock composition was estimated to contain 77% dolomite, 16.4% tremolite, and 6.6% calcite in the tremolite zone, according to the observed modal compositions of the sample. Reaction progress in the internally buffered system can be calculated using the equilibrium value of X_{CO_2} at a given temperature following Ferry (1991), using the stoichiometry of reaction 1:

$$\xi = \frac{X_{CO_2} n_{CO_2}^{initial} + X_{CO_2} n_{H_2O}^{initial} - n_{CO_2}^{initial}}{9 - 10 X_{CO_2}} \quad (3)$$

The amount of calcite produced is subsequently divided by the number of grains in the reference volume. This number fits the observed typical crystal size (Fig. 9). The grain diameter equals the observed grain diameter of 400 µm. The Mg distribution is then modeled as a one-dimensional profile on the central plane of the assumed spherical crystal.

Modeling results revealed that the reaction went to completion near the invariant point at about 585 °C. This temperature corresponds to the peak temperature estimated by our thermal models for the selected sample after ~15 000 years. The model predicts a concentric Mg-zoning profile for a central cut of

a spherical calcite grain grown along the prograde path (Fig. 10). After an initial growing stage, where calcite is formed at about 490 °C, a sharp increase in X_{Mg} is observed until the grain reaches a size of ~80 µm. This is the result of the steep slope of the reaction in the T-X_{CO_2}-diagram during that stage. Subsequent growth at elevated temperatures produces the biggest part of the grain, with a nearly flat X_{Mg} toward the grain rim. The X_{Mg} value in the outermost part of the grain represents the last growth stage of the crystal and thus the peak temperature of the contact metamorphic event. It has to be noted that the reaction progress depends on the change of X_{CO_2} and thus one could also imagine a case were the reaction went to completion, but the temperature further increases. The large fraction of calcite produced during the last stage is due to the shape of reaction 1 in T-X_{CO_2} space (Fig. 7). This geometry dictates that as temperature increases, progressively more CO_2 (and thus calcite) is produced with the same increment of temperature increase.

Modeled Mg distributions were transformed into histograms to compare the results with the measurements. The modeled Mg profile shown in Figure 10a only represents a central cut through the crystal. However, crystals present in thin sections are randomly cut. Hence, the modeled X_{Mg} profile for the central plane has to be weighted in terms of crystal intersection probability. This was numerically achieved by calculating the Mg distribution for 500 cutting planes for the modeled sphere. Each cutting plane has an equal probability to be measured. Thus, summing up a sufficiently large enough number of possible planes results in a representative and unique solution for the modeled calcite grain. To compare the modeled Mg composition of calcite with our natural data set, the calculated Mg profiles on each plane were transformed into probabilities for a X_{Mg} value to be measured. This was done by dividing the cutting planes into areas with equivalent ranges in X_{Mg} values, corresponding to the bins in the histogram. The bin size was chosen to be same as those used for the natural samples. Summing up the areas for each bin for the 500 planes and normalizing those results in a probability histogram that allows for direct comparison to natural samples.

The histogram obtained for a calcite crystal grown along a prograde T-t path and in which growth zoning is the only process affecting the Mg distribution is shown in Figure 10b. This probability distribution is highly skewed toward the highest X_{Mg}-value (skewness = –3.60); nearly 80% of the measured values are predicted to fall within the bin representing the highest X_{Mg} values, and thus peak temperature. Measurements with the highest X_{Mg} values have a high probability because lower X_{Mg} values are limited to a small region nearly through the center of the crystal. Thus, these low values will be measured only if a grain is cut through or at least near its central plane. The distribution is too narrow compared to natural samples. In addition, minerals should be concentrically zoned, which is not observed in our natural samples. Hence, prograde growth zoning alone cannot explain the observed variations in natural samples (Figs. 3–5).

Calcite growth by mixed volatile reaction in a closed system with diffusion

The growth model described above was extended to include intracrystalline diffusion. The diffusion in spherical coordinates was calculated using Fick's second law:

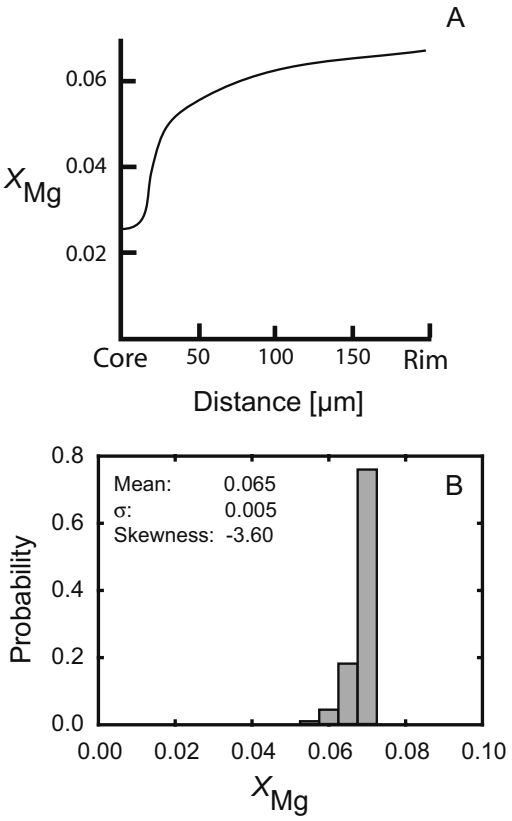

FIGURE 10. Modeled X_{Mg} profile for a central cut of a calcite grown by the reaction 1 in a closed system. Note that the prograde X_{Mg} signature is only recorded near the center of the grain. The histogram shows the probability of an X_{Mg} value to be measured taking into account intersection probabilities of spherical calcite grains in a thin section. The high probabilities of measuring the outer parts of the grains lead to highly skewed distributions, which do not agree with distributions measured in natural samples (Fig. 3).

$$\frac{\partial c}{\partial t} = D\frac{\partial^2 c}{\partial r^2} + \frac{2D}{r}\frac{\partial c}{\partial r} \tag{4}$$

where c is the Mg concentration, r is the radius of the growing sphere, and t is the time. The diffusion coefficient was calculated by the Arrhenius equation:

$$D = D_0 e^{-Q/RT} \tag{5}$$

where D_0 is the pre-exponential diffusion factor, Q is the activation energy. T is the absolute temperature, and R is the universal gas constant. The pre-exponential factor and the activation energy for Mg diffusion in calcite were taken from the experimentally derived data (Kent et al. 2001) with log D_0 = –16.0 m²/s and Q = 76 kJ/mol. However, additional runs using alternative published rate data for Mg diffusion in calcite (e.g., Fisler 1999) have been shown to produce very similar results for modeled T-t path in this study. The modeling domain extends from the center of the grain to its grain boundary. The size of the domain therefore increases with time because of the continuous calcite growth. We chose a standard no-flow boundary condition for the center,

whereas the Mg concentration at the grain boundary was fixed at its equilibrium value for the temperature at any time. The diffusion equation was solved numerically using a Crank-Nicholson scheme (Crank 1975).

Extending the growth model by volume diffusion, results in an Mg profile for a central-cut calcite crystal as shown in Figure 11a. Using the same growth conditions as in the previous model, the original low X_{Mg} values in the center of the grain are nearly completely reset by diffusion because growth of the calcite grain along the prograde path is relatively slow compared to diffusion, even for this contact metamorphic *T-t* path. Diffusion will affect the grain further after grain growth stops, during subsequent cooling. Consequently, the outermost parts of the grain will become zoned, with progressively lower X_{Mg} values toward the grain edge. Since intersections in the outer part of the grain cover larger areas in the cut planes, the lower values in this region will have a stronger effect on the resulting histogram. Compared to the case of no diffusion, the calculated histogram for this model of growth and diffusion shows greater total variations in X_{Mg}, and the values of X_{Mg} that are slightly lower than peak values now have the highest probability (Fig. 11b). The high measurement probability in the outer part of the grain with significantly lower X_{Mg} values leads to these larger variations in the X_{Mg} values. The histogram approaches a Gaussian shape, as indicated by a smaller skewness of –2.7. The high values corresponding to the highest temperature are still dominant ($\sigma = 0.005$) and only slightly modified. Using the maximum value yields a temperature of 580 °C, which gives a reasonable approximation of peak temperature.

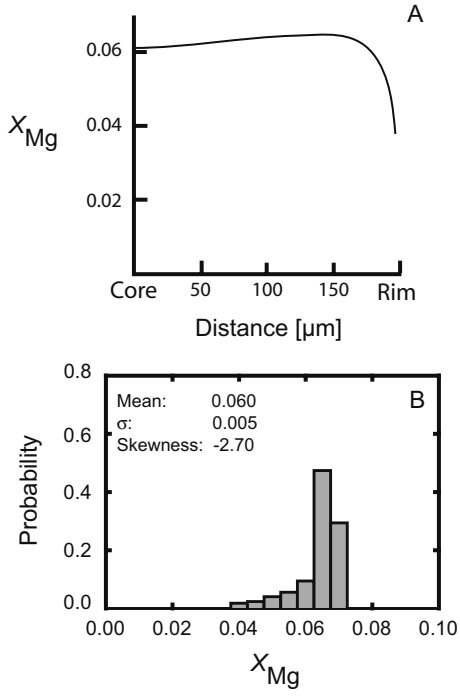

FIGURE 11. Modeled X_{Mg} profile for a central cut of a calcite grown by the reaction 1, which is altered by volume diffusion along the *T-t* path for the Ubehebe Peak aureole. Diffusion nearly erases the prograde X_{Mg} signature, and the outer part of the grain shows significantly lower X_{Mg} values. The probability histogram is still skewed toward X_{Mg} values representing peak *T*, and does not match the natural case.

Calcite growth by fluid-driven, mixed-volatile reaction with diffusion

Results from the first model (thermally activated calcite growth, no diffusion) reveal that only the innermost part of the crystal will preserve the original low Mg signature from the early part of the prograde *T-t* path. The most straightforward way to increase the development and preservation of the original low Mg signature is to allow for more calcite growth during the early stages of the *T-t* path. This approach can be justified for contact aureoles where mineral reactions are likely driven by fluid infiltration (Ferry 1988, 1991, 1996a, 1996b; Labotka et al. 1988; Baumgartner and Ferry 1991; Cook et al. 1997; Roselle et al. 1999). Most reactions in the siliceous carbonate system can be driven by infiltration of a fluid phase. Stable isotope analyses of carbonates and silicates in the Ubehebe Peak aureole revealed that magmatic fluids infiltrated the aureole (Roselle 1997; Roselle et al. 1999; Müller et al. 2004). If the magmatic fluid was the only fluid present in the host rocks, this would dramatically change the reaction path of the system. The interpretation of an infiltration driven system is also supported in the field by the absence of a well-defined diopside zone in the Ubehebe Peak contact aureole.

In this third set of models, calcite grains were assumed to grow instantaneously at a given temperature to their final size (400 µm). At the time of formation, the entire calcite grain is homogeneous and has the equilibration X_{Mg} value defined by the temperature of formation. Subsequently, only diffusion will affect Mg distribution of the crystal along the rest of the *T-t* path. In a first run, calcite is assumed to grow at 425 °C, which corresponds to a calcite formed by the tremolite-producing reaction (Fig. 7). Results reveal that the original lower X_{Mg} composition is largely preserved in the grain interior. Subsequent diffusion along the prograde path increased the Mg content in progressively wider segments of the exterior part of the grain with time (Fig. 12a). Diffusion during cooling subsequently decreased the Mg content near the grain boundary again. No X_{Mg} values record the peak temperature. The resulting histogram mimics a near Gaussian distribution (Fig. 12b) with a small skewness of –0.28. The mean value of $X_{Mg} = 0.045$ corresponds to the mean value observed in natural samples of the tremolite zone, but even the highest value ($T = 550$ °C) in the histogram (Fig. 12a) significantly underestimates the peak temperature (585 °C) that the calcite grain experienced.

A second model assumed a calcite crystal growing at peak temperature (585 °C) due to infiltration. In this case, only retrograde diffusion will affect the Mg composition of the calcite grain. As a consequence the original Mg content at the crystallization temperature is preserved over a large part of the grain interior (Fig. 12c). Only the outermost 40 µm of the crystal exhibit lower Mg contents owing to diffusion during cooling. Consequently, the resulting histogram (Fig. 12d) shows a large probability of measuring the highest X_{Mg} value. Nevertheless, measured probabilities enhance representation of the outer part of the grain and lead to significant variance in the histogram ($\sigma = 0.01$), but a Gaussian distribution is not produced (skewness = –2.4).

The two models presented above represent end-member cases since each calcite crystal growing under prograde conditions will fall in the range between mineral growth at very early stages (Fig. 12a) and growth at peak metamorphic conditions (Fig. 12c).

In another model, we assumed retrograde calcite growth during cooling at 500 °C. As in the previous case, the Mg content of the calcite grain is only affected by retrograde diffusion. Lower X_{Mg} values are only observed in the very outermost part of the grain since diffusion becomes slower with decreasing temperature. Thus, the original Mg content at the crystallization temperature is preserved over nearly the entire grain (Fig. 12e). The resulting histogram therefore exhibits only a very small variance ($\sigma = 0.001$) and an extreme negative skewness of –5.68 (Fig. 12f).

The models presented so far result in calculated histograms that reproduce approximately the shape and distribution of X_{Mg} values of the histograms from the natural data. However, all models predict concentric zoning patterns in X_{Mg}, whereas little systematic compositional zoning within calcite grains was found in the natural samples.

Effects of submicroscopic exsolution lamellae

Exsolution lamellae are commonly observed in calcites (Goldsmith 1960; Nesbitt and Essene 1982). A calcite equilibrated at peak temperature will contain excess Mg upon cooling if it cannot equilibrate. This excess Mg is eventually exsolved from the crystal lattice of calcite to form lamellae of essentially pure dolomite. Grains with visible exsolution lamellae are commonly excluded for use in calcite-dolomite thermometry. Nevertheless, they could be reintegrated over the whole grain to obtain a reasonable temperature (Hutcheon and Moore 1973; Treiman and Essene 1984). Our measurements of the Mg content of calcite were obtained by spot analyses with a beam diameter of at least 15 µm. Hence, the measured Mg content is the integrated value for the area of the spot. Assuming that microscopic exsolution lamellae exist but are too small to be visible (<0.8 µm), the measured (integrated) X_{Mg} value will vary depending on the number and thickness of lamellae within the analyzed spot area. Lamellae larger then 0.8 µm would be visible and crystals containing them would have been avoided during analysis. Lamellae that are very small compared to the spot size will result in a large number of lamellae within the area covered by the spot. As a consequence, each analysis would contain roughly the same amount of lamellae and thus no variation occurs (Fig. 13b).

To quantify the effect of small lamellae on the variations of measured X_{Mg} values, we assumed a calcite grain 400 µm across that equilibrated at 620 °C ($X_{Mg} = 0.079$). Subsequent cooling down to 450 °C produced excess Mg that was distributed on equally spaced lamellae (Fig. 13). Since the amount of excess Mg is fixed by the size of the grain and the chosen temperatures, the

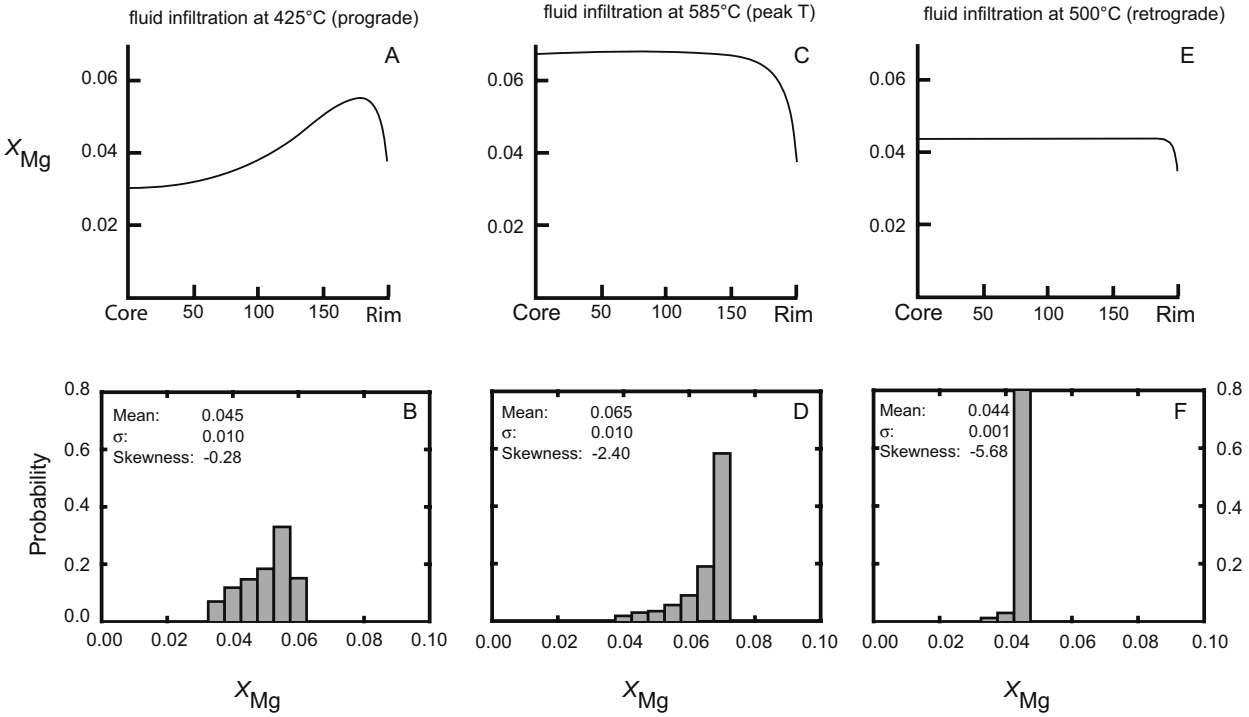

FIGURE 12. Modeled X_{Mg} profiles for central cuts of calcite crystals produced during infiltration-driven, mixed-volatile reactions including diffusion. (**a**, **b**) Infiltration at tremolite grade. Diffusion causes significantly elevated X_{Mg} values at the outer part of the grain, but retrogression erases the X_{Mg} values representing peak *T*. The resulting probability histogram of X_{Mg} values to be measured in a spherical calcite grain agrees well with measured distributions of X_{Mg} values (Fig. 3). (**c**, **d**) Infiltration at peak *T*. The crystallization X_{Mg} value at peak *T* is preserved over a large part of the grain. Diffusion led to lower X_{Mg} values near the grain boundary. As a result, the probability histogram is skewed but exhibits significant variations. (**e**, **f**) Infiltration during cooling. Lower X_{Mg} values due to diffusion are limited to a narrow region near the grain boundary and consequently the resulting probability histogram exhibit only small variations in disagreement with natural samples.

lamellae size and their spacing can be varied as a function of its number. Further simplifying, we assumed that the composition of the matrix and the lamellae are each constant for the grain after cooling. In addition, we assume that lamellae are equally spaced. Thus, the area covered by a lamellae has an X_{Mg} value of pure dolomite (X_{Mg} = 0.5) and the rest of the grain is set to the equilibrated X_{Mg} value of 0.0335 for 450 °C. Microprobe analyses were simulated on a straight profile perpendicular to the lamellae by integrating areas of lamellae and calcite host over the spot size (Fig. 13). Each simulated microprobe spot analysis has an equal probability of being measured. A large number of analyses were simulated to statistically obtain the probability for the measured X_{Mg} values.

In the first calculation, we used a spot size of 10 µm. The number of possible compositionally distinct analyses is defined by the size of the lamellae (the thicker the lamellae the greater the distance between two identical points). As discussed above, very small sizes of the lamellae (<0.3 µm) will not disturb the analyses. Their high abundances within the analyzed area become statistically uniform and measured values give only the original value of the peak temperature (Fig. 14a). The presence of lamellae start producing analytical variations as the size of the lamellae increases above 0.3 µm. Analyses containing higher proportions of lamellae will exhibit X_{Mg} values higher than the value defined by peak temperature. In contrast, analyses dominated by the area of the re-equilibrated calcite matrix will show lowered values (Figs. 14b and 14c). However, the histogram does not mimic a Gaussian distribution. With increasing lamellae size, the scatter becomes larger. In a second set of calculations, we increased the spot size to 15 µm in diameter. As with the first set of calculations, an effect can be seen at a lamellae size of about 0.5 µm. (Fig. 14b). Further increase of lamellae size enlarges the variations. Two probability peaks develop with one peak consisting principally of the calcite matrix composition, the other of the dolomite lamellae, respectively. Consequently, the resulting histogram converges to a bimodal distribution (Fig. 14f).

The calculations demonstrate that the presence of microscopic exsolution lamellae can produce significant variations in the measured Mg content of a calcite grain. Because of the spatial distribution of lamellae, no systematic trend will be observed and the measured values appear arbitrarily distributed, even for an initially zoned grain. The presence of such submicroscopic exsolution lamellae can potentially make substantial contributions to the development of nearly Gaussian type shapes. By contrast, the limited scatter in most combinations of spot and lamellae size suggests that this process can be only part of the process creating the observed variations (Figs. 2, 3, and 5).

In a third set of calculations, we combined the exsolution model with the Mg-distributions obtained for infiltration driven calcite growth with subsequent diffusion (Fig. 15). We assume the rock cooled down to 400 °C when the submicroscopic exsolution lamellae with a size of 0.3 µm formed. Resulting probability histograms are shown in Figure 15. Calcite compositions in calcite grains grown at low temperatures, in the tremolite zone, are only modestly affected by the formation of submicroscopic exsolution lamellae, since the amount of excess Mg is too small to produce a significant amount of lamellae. In contrast, the probability distribution for X_{Mg} values measured in calcite grains grown near peak temperature is clearly shifted toward a Gaussian shape indicated by a smaller skewness of only –0.7. The mean value also decreases to X_{Mg} = 0.056. Thus, it is smaller than the values observed in natural samples of the forsterite zone (Table 5).

Consequences of calcite-dolomite thermometry at Ubehebe Peak

The measured Mg content of metamorphic calcite crystals exhibit large variations. Variations at the scale of a thin section as well as multiple analyses within single grains both reveal that significant re-equilibration occurred, warranting either the use of 2σ (Roselle 1997) or the approach using the maximum measured X_{Mg} value (Cook and Bowman 1994). However, in this study we were able to correlate analyses of individual calcite grains with adjacent silicate minerals in the natural samples (Fig. 4). Furthermore, the spatial variability of the Mg content of calcite on a thin section scale indicates that growth of tremolite and forsterite were driven by fluid flow. This result is in agreement with phase petrology and stable isotope geochemistry (Roselle

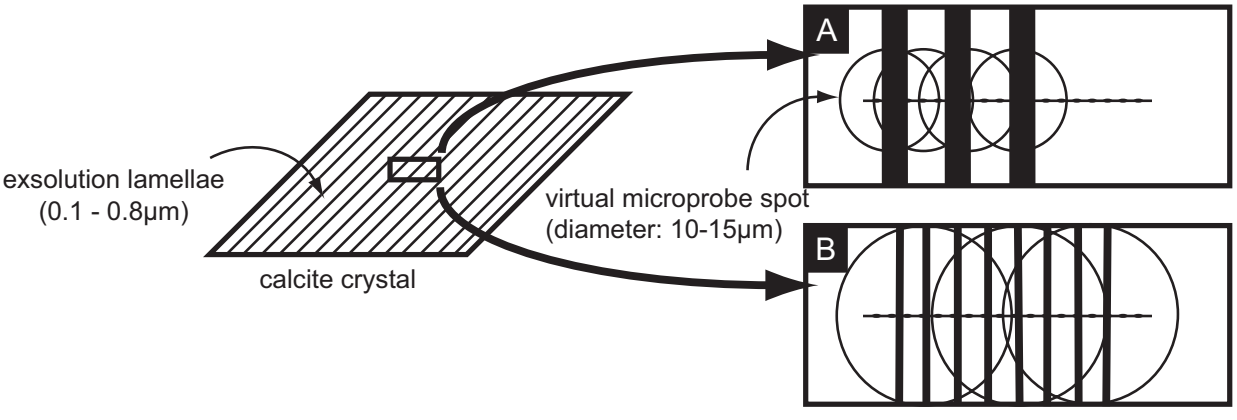

Figure 13. Schematic illustration of the effect of submicroscopic exsolution lamellae on microprobe analyses. (**a**) The measured X_{Mg} value is the result of the average composition activated by the microprobe beam. (**b**) Very small lamellae sizes will not cause variations in the measured X_{Mg} values, since every spot contains roughly the same amount of dolomite exsolution lamellae.

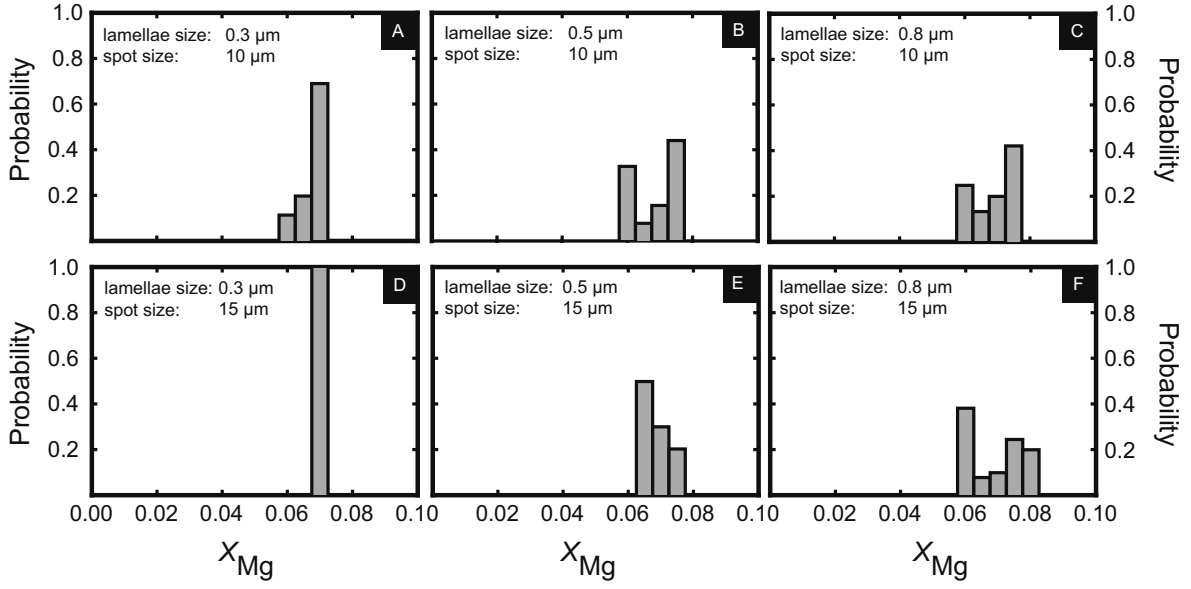

FIGURE 14. Probability histograms of measured X_{Mg} values as a function of different sizes of exsolution lamellae and virtual microprobe spot size. The calcite grain is assumed to have grown entirely at peak T (620 °C) and subsequently cooled down to 400 °C. Very fine lamellae have no significant effect and the crystallization X_{Mg} value is measured (**a**, **d**). Increasing lamellae size causes large variations including X_{Mg} values higher than the original crystallization Mg content (**b**, **e**). A bimodal distribution is approached where the microprobe spot is either dominated by exsolution lamellae or equilibrated calcite host (**c**, **f**).

TABLE 5. Statistical analyses of modeling results for the probability of X_{Mg} values to be measured

	Descriptive statistics		
Run conditions	Average	Std Dev	skewness
cont. growth, no diff, no exsol	0.065	0.005	–3.60
cont. growth, diff, no exsol	0.060	0.005	–2.70
rapid growth (425 °C), diff, no exsol	0.045	0.010	–0.28
rapid growth (585 °C), diff, no exsol	0.065	0.010	–2.40
rapid growth (500 °C), diff, no exsol	0.044	0.001	–5.68
rapid growth (425 °C), diff, exsol	0.044	0.007	–0.66
rapid growth (585 °C), diff, exsol	0.056	0.011	–0.70
rapid growth (combined), diff, exsol	0.051	0.011	–0.58

Notes: The statistical treatment of modeled Mg distributions within a spherical calcite grain takes also into account the intersection probabilities.

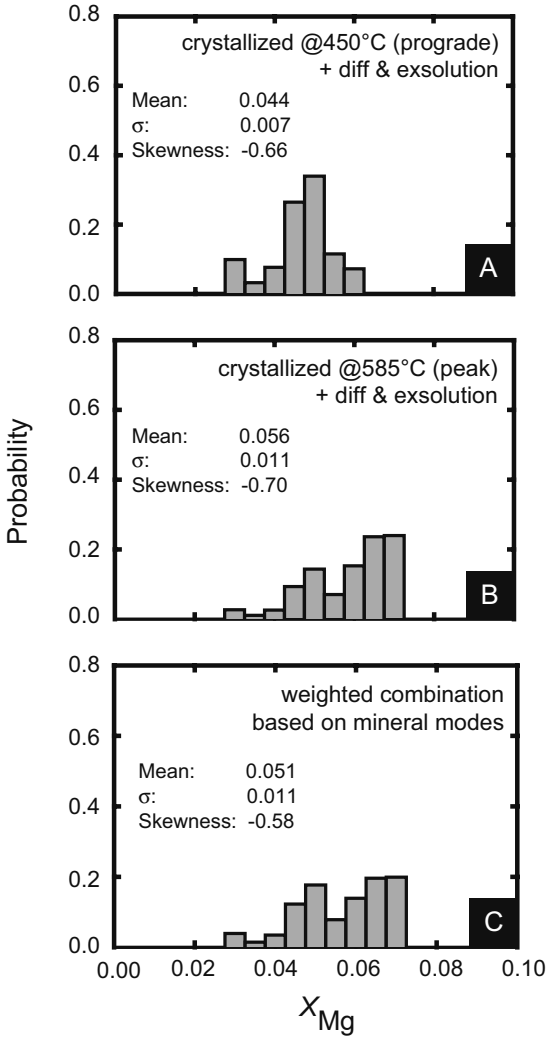

►**FIGURE 15.** Probability histograms of measured X_{Mg} values for calcite grown during infiltration-driven mixed-volatile reactions including diffusion and exsolution lamellae. The predicted Mg content probability of grains grown with tremolite zone matches the near-Gaussian shape observed in natural samples, albeit somewhat shifted to lower values. The highly skewed distribution obtained in Figure 12 for crystals grown at peak T is shifted toward lower X_{Mg} values and converges to a Gaussian shape. A combination of both distributions based on the mineral modes observed in natural samples of the Ubehebe Peak result in an Mg distribution that is in excellent agreement with those obtained in natural samples (Fig. 3).

et al. 1999; Müller et al. 2004). We interpret fluid infiltration to have initiated reactions at the Ubehebe Peak during heating.

Results show that the original lower Mg content is maintained in a significant fraction of the grain interior (Fig. 12) for models where calcite is assumed to grow instantaneously because of fluid infiltration. The Mg content is strongly changed near the grain boundaries due to diffusion. As a result, the calculated histogram of the model reproduces reasonably well the variations observed in natural samples. Note that an important assumption of our model is fast diffusion along the grain boundaries. Calcite in halos surrounding the porphyroblasts commonly appears in clusters. Dry grain boundaries would significantly decrease diffusion rates and hence the flux of Mg into the interior of the cluster. Hence, the calculated effect of diffusion on the Mg composition of calcite grains has to be regarded as a maximum.

Modeling results for fluid-driven, rapid calcite growth at low temperatures corresponding to the tremolite-forming reaction are in excellent agreement with measured distribution of Mg contents of calcite samples collected in the tremolite zone. In contrast, the modeled X_{Mg} distribution for calcites that grew during retrograde growth of tremolite does not match the observed variations. We conclude that most tremolite crystals were formed during heating, on the prograde path. The infiltration of a fluid phase can apparently cause significant overstepping of stable reactions for a short time and produce rapid growth of porphyroblasts and associated calcite halos. Rapid crystal growth is also indicated by the narrow range of temperatures recorded by calcite grains within single halos along forsterite porphyroblasts (Fig. 8).

All of the above models result in concentric zoning patterns. The presence of such zoning has been described by Wada and Suzuki (1983). However, detailed analyses of samples from the Ubehebe Peak area do not exhibit systematic zoning. The formation of submicroscopic exsolution lamellae during cooling would produce randomly distributed higher and lower measured X_{Mg} values within individual grains, masking the pre-existing systematic zoning patterns. Very high measured X_{Mg} values that yield unrealistically high temperatures may be the result of incorporation of a significant number of dolomite lamellae within the microprobe spot. The use of maximum X_{Mg} values to calculate temperatures would then overestimate the metamorphic peak temperature, and a 2σ approach seems more prudent.

Acknowledgments

This study is part of the first author's Ph.D. thesis. Financial support was provided by grant 2100-066996 from the Swiss National Science Foundation. Comments and discussions with J.R. Bowman, M. Cosca, T.W. Vennemann, and D. Trail on earlier versions helped to improve the quality of the manuscript. We thank Ted Labotka and an anonymous reviewer for their insightful and constructive comments as well as M. Gottschalk for the editorial handling.

References cited

Anovitz, L.M., Essene, E.J., Goldsmith, J.R., and Heard, H.C. (1987) Phase equilibria in the system $CaCO_3$-$MgCO_3$-$FeCO_3$. Journal of Petrology, 28, 389–414.

Baumgartner, L.P. and Ferry, J.M. (1991) A model for coupled fluid-flow and mixed-volatile mineral reactions with applications to regional metamorphism. Contributions to Mineralogy and Petrology, 106, 273–285.

Carlson, W.D. (2002) Scales of disequilibrium and rates of equilibration during metamorphism. American Mineralogist, 87, 185–204.

Carlson, W.D., Denison, C., and Ketcham, R.A. (1995) Controls on the nucleation and growth of porphyroblasts: Kinetics from natural textures and numerical models. Geological Journal, 30, 207–225.

Connolly, J.A.D. and Kerrick, D.M. (1987) An Algorithm and computer-program for calculating composition phase-diagrams. Calphad-Computer Coupling of Phase Diagrams and Thermochemistry, 11, 1–55.

Cook, S.J. and Bowman, J.R. (1994) Contact-metamorphism surrounding the alta stock—thermal constraints and evidence of advective heat-transport from calcite plus dolomite geothermometry. American Mineralogist, 79, 513–525.

Cook, S.J., Bowman, J.R., and Forster, C.B. (1997) Contact metamorphism surrounding the alta stock: Finite element model simulation of heat- and $^{18}O/^{16}O$ mass-transport during prograde metamorphism. American Journal of Science, 297, 1–55.

Crank, J. (1975) The Mathematics of Diffusion, 414 p. Oxford University Press, New York.

Essene, E.J. (1983) Solid solutions and solvi among metamorphic carbonates with applications to geologic thermobarmetry. In R.J. Reeder, Ed., Carbonates: Mineralogy and Chemistry, 11, p. 77–96. Reviews in Mineralogy, Mineralogical Society of America, Chantilly, Virginia.

Evermann, R.L. (1998) A textural and microfabric analysis of the deformation at Ubehebe Peak contact aureole, Death Valley National Park, California. M.S. thesis, University of Wisconsin, Madison.

Ferry, J.M. (1988) Infiltration-driven metamorphism in northern New England, U.S.A. Journal of Petrology, 29, 1121–1159.

——— (1991) Dehydration and decarbonation reactions as a record of fluid infiltration. In D.M. Kerrick, Ed., Contact Metamorphism, 26, p. 351–393. Reviews in Mineralogy, Mineralogical Society of America, Chantilly, Virginia.

——— (1996a) Prograde and retrograde fluid flow during contact metamorphism of siliceous carbonate rocks from the Ballachulish aureole, Scotland. Contributions to Mineralogy and Petrology, 124, 235–254.

——— (1996b) Three novel isograds in metamorphosed siliceous dolomites from the Ballachulish aureole, Scotland. American Mineralogist, 81, 485–494.

——— (2001) Calcite inclusions in forsterite. American Mineralogist, 86, 773–779.

Ferry, J.M. and Dipple, G.M. (1992) Models for coupled fluid flow, mineral reaction, and isotopic alteration during contact metamorphism: The Notch Peak aureole, Utah. American Mineralogist, 77, 577–591.

Ferry, J.M. and Gerdes, M.L. (1998) Chemically reactive fluid flow during metamorphism. Annual Review of Earth and Planetary Sciences, 26, 255–287.

Fisler, D.K. (1999) Diffusion of Ca and Mg in calcite. American Mineralogist, 84, 1392.

Goldsmith, J.R. (1960) Exsolution of dolomite from calcite. Journal of Geology, 68, 103–109.

Goldsmith, J.R. and Heard, H.C. (1961) Subsolidus phase relations in the system $CaCO_3$-$MgCO_3$. Journal of Geology, 69, 45–74.

Holland, T. and Powell, R. (2001) Calculation of phase relations involving haplogranitic melts using an internally consistent thermodynamic dataset. Journal of Petrology, 42, 673–683.

Holness, M.B., Bickle, M.J., and Graham, C.M. (1991) On the Kinetics of Textural Equilibration in Forsterite Marbles. Contributions to Mineralogy and Petrology, 108, 356–367.

Hutcheon, I. and Moore, J.M. (1973) Tremolite Isograd near Marble-Lake, Ontario. Canadian Journal of Earth Sciences, 10, 936–947.

Joesten, R.L. (1991) Kinetics of coarsening and diffusion-controlled mineral growth. In D.M. Kerrick, Ed., Contact Metamorphism, 26, p. 507–582. Reviews in Mineralogy, Mineralogical Society of America, Chantilly, Virginia.

Kent, A.J.R., Hutcheon, I.D., Ryerson, F.J., and Phinney, D.L. (2001) The temperature of formation of carbonate in Martian meteorite ALH84001: Constraints from cation diffusion. Geochimica et Cosmochimica Acta, 65, 311–321.

Kretz, R. (1983) Symbols for rock-forming minerals. American Mineralogist, 68, 277–279.

Labotka, T.C., Nabelek, P.I., and Papike, J.J. (1988) Fluid Infiltration through the Big Horse Limestone Member in the Notch Peak Contact-Metamorphic Aureole, Utah. American Mineralogist, 73, 1302–1324.

Lasaga, A.C. (1998) Kinetic theory in earth sciences, 728 p. Princeton University Press, New Jersey.

Letargo, C.M.R., Lamb, W.M., and Park, J.S. (1995) Comparison of calcite plus dolomite thermometry and carbonate plus silicate equilibria—constraints on the conditions of metamorphism of the Llano Uplift, Central Texas, U.S.A. American Mineralogist, 80, 131–143.

Masch, L. and Heuss-Abichler, S. (1991) Decarbonation reactions in siliceous dolomites and impure limestones. In G. Voll, J. Töpel, D.R.M. Pattison, and F. Seifert, Eds., Equilibrium and Kinetics in Contact Metamorphism. The Ballachulish Ingneous Complex and its Aureole, p. 211–227. Springer, New York.

McAllister, J.F. (1955) Geology and mineral deposits in the Ubehebe Peak Quadrangle, Inyo County, California, p. 63. California Division of Mines and Geology, San Francisco.

——— (1956) Geology of the Ubehebe Peak Quadrangle, California, U.S.A. Geological Survey, San Francisco.

Müller, T. (2002) Structural and petrological study of the northern Ubehebe Peak contact aureole, Death Valley National Park, California, U.S.A. Diploma thesis, University of Mainz, Germany.

Müller, T., Baumgartner, L.P., Foster Jr., C.T., and Vennemann, T.W. (2004) Metastable prograde mineral reactions in contact aureoles. Geology, 32, 821–824.

Nesbitt, B.E. and Essene, E.J. (1982) Metamorphic thermometry and barometry of a portion of the southern Blue Ridge Province. American Journal of Science, 282, 701–729.

Powell, R., Condliffe, D.M., and Condliffe, E. (1984) Calcite-dolomite geothermometry in the system $CaCO_3$-$MgCO_3$-$FeCO_3$—an experimental study. Journal of Metamorphic Geology, 2, 33–41.

Rathmell, M.A., Streepey, M.M., Essene, E.J., and Van Der Pluijm, B.A. (1999) Comparison of garnet-biotite, calcite-graphite, and calcite-dolomite thermometry in the Grenville Orogen, Ontario, Canada. Contributions to Mineralogy and Petrology, 134, 217–231.

Reeder, R.J. (1992) Carbonates—Growth and Alteration Microstructures. In P.R. Buseck, Ed., Minerals and Reactions at the Atomic Scale: Transmission Electron Microscopy, 27, p. 381–424. Reviews in Mineralogy, Mineralogical Society of America, Chantilly, Virginia.

Roselle, G.T. (1997) Integrated petrologic, stable isotopic, and statistical study of fluid-flow in carbonates of the Ubehebe Peak contact aureole, Death Valley National Park, California. Ph.D. thesis, University of Wisconsin, Madison.

Roselle, G.T., Baumgartner, L.P., and Chapman, J.A. (1997) Nucleation-dominated crystallization of forsterite in the Ubehebe Peak contact aureole, California. Geology, 25, 823–826.

Roselle, G.T., Baumgartner, L.P., and Valley, J.W. (1999) Stable isotope evidence of heterogeneous fluid infiltration at the Ubehebe Peak contact aureole, Death Valley National Park, California. American Journal of Science, 299(2), 93–138.

Treiman, A.H. and Essene, E.J. (1984) A periclase-dolomite-calcite carbonatite from the Oka Complex, Quebec, and its calculated volatile composition. Contributions to Mineralogy and Petrology, 85, 149–157.

Wada, H. and Suzuki, K. (1983) Carbon isotopic thermometry calibration by dolomite-calcite solvus temperatures. Geochimica et Cosmochimica Acta, 47, 697–706.

Watson, E.B. (1996) Surface enrichment and trace-element uptake during crystal growth. Geochimica et Cosmochimica Acta, 60, 5013–5020.

——— (2004) A conceptual model for near-surface kinetic controls on the trace-element and stable isotope composition of abiogenic calcite crystals. Geochimica et Cosmochimica Acta, 68, 1473–1488.

Manuscript received February 21, 2007
Manuscript accepted March 10, 2008
Manuscript handled by Matthias Gottschalk